Angular correlation distribution of positron-electron annihilation in GaAs

B. K. Panda*
Institute of Physics, Bhubaneswar 751005, India
(Received 30 November 1992; revised manuscript received 30 September 1993)

Angular correlation of positron annihilation radiations has been measured along the [100], [110], [111], [211], and [221] crystallographic axes in GaAs using the long-slit geometry. A pseudopotential calculation is carried out to understand the experimental data. There is good agreement between experimental and theoretical data. The structures seen in the low-momentum region of the data are interpreted in terms of the σ and π bonds of the sp^3 hybridized bonding orbitals. The experimental data when compared with the calculated data reveal the presence of electron-positron many-body correlation effects.

I. INTRODUCTION

Angular correlation of positron annihilation radiation (ACPAR) gives information about the electron momentum distributions in solids.[1] Long-slit ACPAR gives the one-dimensional (1D) projection of the electron momentum density (EMD) by integrating the annihilation rate over a plane. On the other hand 2D ACPAR, which gives the integrated rate over an axis, produces more detailed information about the EMD of solids. A number of ACPAR studies have been carried out in covalent elemental semiconductors, viz., Si and Ge by different groups.[2–8] Since compound semiconductors are covalent materials with a degree of ionicity, they are expected to show different behavior compared to group IV semiconductors because the probability of the positron annihilating with the negative ion is greater than that with the positive ion.[9] The 1D ACPAR data of GaP,[10] GaSb,[11] GaAs, InP, InAs, and InSb (Ref. 12) however, show similar behavior to Si and Ge. In all the measurements the data along [100] and [110] directions show a dip in the low momentum region and a sharp peak along the [111] direction. The 3D EMD in Si, Ge, GaAs, InP, and GaSb, measured recently by Kondo *et al.*, show the same behavior as in 1D ACPAR data.[13] It is also observed in 1D and 2D ACPAR data that the dips are somewhat shallow in InP and GaSb compared to Si, Ge, GaP, and GaAs. The analysis by Kondo *et al.* for the origin of the ACPAR structures is based on the group theory. They argue that the wave function whose representation is totally symmetric under any operation of the space group at a given point of the wave vector in the Jones zone does not contribute any feature to the EMD. Since the positron wave function is in the lowest energy state, it is totally symmetric and hence does not contribute any feature to the EMD. Likewise the electron wave functions belonging to the lower two valence bands in Si and Ge do not contribute any feature. Therefore the features at the low momentum region are due to the nonsymmetric upper two valence bands. The high O_h^7 symmetry in group IV semiconductors lowers to T_d^2 symmetry in III-V semiconductors. As a result of this some extra bands become invariant under any operation belonging to the space group of the crystal in III-V semiconductors. This makes III-V semiconductors like GaSb and InP more isotropic compared to group IV semiconductors. However, since the degree of distortion in GaAs is less because both the elements of GaAs belong to the same row in the Periodic Table and contribute the same type of orbitals ($4p$) to the bonding the prominent features found in Si and Ge are also observed in GaAs.

This explanation leaves a few questions in mind. It is well known that the Compton profile (CP) method is another powerful tool for obtaining the information about the EMD of solids.[1] Following the analysis of Kondo *et al.*,[13] one finds no difference in EMD obtained from ACPAR and CP data because the positron wave function does not contribute any feature to it. The positron wave function however is highly anisotropic in the interstitial region and changes the behavior of the low momentum region of the ACPAR data significantly when compared to high resolution CP data.[14] We observe prominent anisotropy in GaP in spite of its elements not belonging to the same row in the Periodic Table. The II-VI semiconductor ZnSe with similar T_d^2 symmetry to GaAs has the same lattice constant as in Ge and GaAs. The CP anisotropies in Ge, GaAs, and ZnSe show however that the anisotropies become smaller in the order Ge, GaAs, and ZnSe which is consistent with their ionic trend in bonding character.[15]

The main aim of this paper is to propose a different analysis than that presented by Kondo *et al.* to understand the origin of the structures in the momentum distributions in the low momentum region. The experimental and theoretical CP data are available along several crystallographic directions of GaAs.[16] In the present work we have taken the measured and calculated long-slit ACPAR data along the same directions of GaAs. Comparison of the ACPAR data with the CP data will reveal the effect of the positron wave function on the momentum density. The contribution of the electron-positron many-body correlation effect on the EMD of GaAs will also be discussed because in lifetime analysis it is predicted to be the same as in Ge.[17]

The organization of this paper is as follows. We give a brief account of our measurement procedure and data analysis in Sec. II. In Sec. III we explain our theoretical

procedure. In Sec. IV the measured and calculated data are compared and discussed. We conclude in Sec. V.

II. EXPERIMENT

We shall only give a short account of the experimental procedure which has been discussed in detail elsewhere.[18] The samples with plane faces cut perpendicular to [100], [110], [111], [211], and [221] directions were obtained from MCP, Electronic Materials Ltd., England. Samples were 15 mm×10 mm×3 mm in size. Since the positron depth profile contributes some asymmetry to the long-slit ACPAR data,[19] we reduced the thickness of all the samples to 0.5 mm. Since the imported samples contained as-grown point defects which can contribute substantially to the observed EMD, the samples were annealed in arsenic atmosphere at 800 °C for half an hour to remove these defects. The samples were then chemically etched and diamond polished to remove surface oxidation effects. Long-slit ACPAR measurements were carried out at the Indira Gandhi Centre for Atomic Research at Kalpakkam, India. The details of the experimental setup have been described elsewhere.[20] All the measurements were carried out at room temperature. The 511 keV annihilation γ rays were detected in 30 cm long × 3.8 cm diam NaI(Tl) scintillators at a distance of 3 meters from the position of the sample. The resolving time of the fast-slow coincidence setup was set at 100 nsec. About 4×10^4 counts were collected at the peak of the data in all the directions. The raw data were corrected for chance coincidences, background, and variations in the singles counting at different angular positions of the moving counter following the method of Chiba and Tsuda.[21] The momentum resolution of the spectrometer was 1.3 mrad. Since this resolution is rather large compared to the conventional long-slit ACPAR measurements, we have deconvoluted the raw data using the fast Fourier transform method described elsewhere.[18] Since the deconvoluted data were found to be symmetric about the zero momentum position, they were folded and their area was normalized to unity from 0 to 2.4 a.u.

III. THEORY

The positron after entering the solid gets thermalized and attracts the surrounding electrons before getting annihilated emitting two γ rays. The coincidence count in the long-slit geometry at momentum p_z is given by

$$N(p_z) = \int_{-\infty}^{\infty}\int_{-\infty}^{\infty} \rho^{2\gamma}(\mathbf{p})dp_x dp_y. \tag{3.1}$$

In the single particle approximation, the two-photon momentum density $\rho^{2\gamma}(\mathbf{p})$ is given by

$$\rho^{2\gamma}(\mathbf{p}) = \sum_{n\mathbf{k}}^{\text{occ.}} \eta_n(\mathbf{k}) \left| \int \Psi_{n\mathbf{k}}(\mathbf{r})\Psi_+(\mathbf{r})\exp(i\mathbf{p}\cdot\mathbf{r})d^3r \right|^2, \tag{3.2}$$

where $\Psi_{n\mathbf{k}}(\mathbf{r})$ and $\Psi_+(\mathbf{r})$ are the electron and positron wave functions, respectively. $\eta_n(\mathbf{k})$ is the occupation probability of the electron at the state n and $\mathbf{k}$. We have not included the electron-positron enhancement factor because its exact form for a semiconductor is not known.

The evaluation of Eq. (3.1) requires both $\Psi_{n\mathbf{k}}(\mathbf{r})$ and $\Psi_+(\mathbf{r})$ to be found from a band structure calculation. Saito, Oshiyama, and Tanigawa,[13] for example, have employed the norm-conserving *ab initio* pseudopotential method to calculate the $\Psi_{n\mathbf{k}}(\mathbf{r})$. We have preferred the empirical pseudopotential scheme for its simplicity and accuracy in reproducing the bands because the pseudopotentials in this scheme are adjusted to fit the measured band gaps.[22] In the present work the nonlocal pseudopotentials of Chelikowsky and Cohen were taken.[23]

Aourag *et al.* have given details of the positron wave function calculation.[9] With the assumption that there is only one positron for many electrons, the positron potential contains the repulsive ion core potential, the attractive Hartree potential, and the electron-positron correlation potential. The electron-positron correlation potential is not included here because its contribution to the total positron potential is quite small as has recently been shown in Ge.[24] In the present case the ion core potential is evaluated in the point core approximation. The Hartree potential is calculated with the occupied electron charge density evaluated from the pseudo-wavefunctions. The positron wave function is represented in terms of a set of plane waves because it does not have any node in the ion core region.

We have employed the Fourier inversion technique, the details of which are given in our earlier paper,[11] to calculate $N(p_z)$ along different crystallographic directions. In this method we calculate the two-photon autocorrelation function (AF) (Ref. 25) defined as

$$B(\mathbf{r}) = \int \rho^{2\gamma}(\mathbf{p})\exp(i\mathbf{p}\cdot\mathbf{r})d^3p. \tag{3.3}$$

In the single particle approximation, $B(\mathbf{r})$ may be derived as

$$B(\mathbf{r}) = \sum_{n\mathbf{k}} \eta_n(\mathbf{k}) \int \Psi^*_{n\mathbf{k}}(\mathbf{r}+\mathbf{r}')\Psi_{n\mathbf{k}}(\mathbf{r}')\Psi^*_+ \times(\mathbf{r}+\mathbf{r}')\Psi_+(\mathbf{r}')d\mathbf{r}'. \tag{3.4}$$

The AF in case of CP data may be obtained by substituting $\Psi_+=1$ in the above expression. The zeros of the AF in the CP analysis for a semiconductor where all bands are filled and $\eta_n(\mathbf{k})$ =const, are seen to have zero passages at lattice translations.[26] The precision of this procedure can be checked by computing $B(r)$ with $\Psi_+=1$ along various axes of the semiconductors and looking at the zero passages along that direction. In an inverse Fourier transform we obtain $N(p_z)$ from $B(z)$ along that direction. The summation over the wave vectors in the occupied Brillouin zone was carried out using the 60-point scheme of Chadi and Cohen.[27] For the evaluation of the electron and positron wave functions, 100 and 300 plane waves were taken, respectively. The core contributions were evaluated and added to the valence $N(p_z)$ after first multiplying by a suitable constant which was obtained by fitting the core profile with the tail of the experimental data. As with the experimental data, the theoretical data were normalized to unity in the range from 0 to 2.4 a.u. to allow for comparison.

IV. RESULTS AND DISCUSSIONS

In this section we present and compare the experimental and theoretical data. The electron-positron many-body effects on the momentum distributions are discussed. Finally the three-dimensional electron momentum density is reconstructed from the experimental and theoretical data.

A. The 2γ momentum distributions

The unit normalized experimental and theoretical ACPAR data along five directions are plotted in Fig. 1. They show good agreement with each other. The low momentum region of the data along [100] and [110] directions are seen to be flat, whereas in the same region the data along [111], [211], and [221] directions are sharply peaked and thus consistent with our earlier observations in GaP (Ref. 10) and GaSb.[11] However, the dips observed in the low momentum region of the experimental data along [100] and [110] directions in Si, Ge,[3,4] and GaAs (Ref. 12) are washed out in the present data because of the inferior momentum resolution of the present experiment. Although we have deconvoluted the experimental data, the dips might have been smeared out by the residual instrumental function. We also observe a break at 0.83 a.u. along the [110] direction.

From Eqs. (3.1) and (3.2) we can see that the nature of the $N(p_z)$ is decided by the **k** summation of the Jones zone and the details of the electron and positron wave functions. Erskine and McGervey[2] have considered the **k** summation by calculating the cross sectional area of the slices through the Jones zone along different directions in Si and Ge. The calculation has shown that the break is at the zone face, but it could not explain the structures at the low and high momentum regions. Inclusion of umklapp components in their model could explain the high momentum regions. The situation in GaAs is the same as in Ge because the Jones zone and the reciprocal lattice vectors are the same in both. The matching of the theoretical data with the measured ones in the high momentum region is because we have included these effects adequately in our calculation.

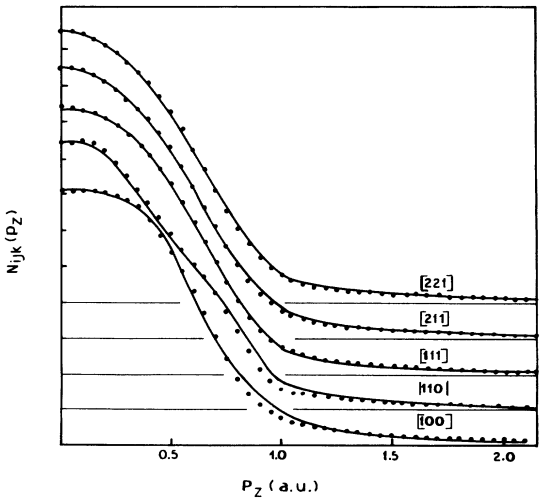

FIG. 1. Experimental (•) and theoretical (−) long-slit ACPAR data along [100], [110], [111], [211], and [221] directions of GaAs.

The success of our calculation over the models of Erskine and McGervey in explaining the low momentum region of the experimental data is due to the fact that we have taken appropriate electron and positron wave functions in our calculation. Because of this the nature of the ACPAR data in the low momentum region can be related to the details of the wave function distributions and their bondings in the interstitial region. In the present case it can be visualized that the nature of the data in the low momentum region is governed by the σ and π bonds of the sp^3 hybridized bonding orbitals. In Si, Pattison, Hansen, and Schneider[28] have shown that there is a $(3p,3p)\sigma$ bond at the first bond length and the interaction of the second neighbor $(3p,3p)\sigma$ bonds is equivalent to introducing a $(3p,3p)\pi^*$ bond between neighboring atoms. From the analysis of Pantelides and Harrison in GaAs,[29] it can be shown that there is a $(4p,4p)\sigma$ bond at the first bond length and a $(4p,4p)\pi^*$ bond at the second bond length. As a result of this there is a strong $(4p,4p)\sigma$ bond along the [111] direction and an admixture of $(4p,4p)\sigma$ and $(4p,4p)\pi^*$ bonds along the [110] direction. Similarly one could also see an admixture of $(4p,4p)\sigma$ and $(4p,4p)\pi^*$ bonds along the [100] direction. In graphite it has been shown that the σ bond makes the profile sharply peaked and conversely that the combination of σ and π bonds creates a dip in the low momentum region.[30] The sharp peaking of the data along the [111] direction and the dip along the [100] and [110] directions are primarily due to the presence of $(4p,4p)\sigma$ and $(4p,4p)\pi^*$ bonds, respectively, along these directions. The effect of the ionic bond on the EMD of GaAs is to reduce the anisotropies and oscillations of the autocorrelation functions when compared to Ge.[8] As mentioned earlier, the shallowing of the dip in GaSb along the [100] direction is because the wave functions in GaSb are more diffused due to its smaller band gap compared to GaP and GaAs.[11]

B. The many-body enhancement effects

Along the [110] direction in Si, Fujiwara, Hyodo, and Ohyama[31] have shown that the ACPAR data are enhanced at the zone face and are dehanced in the high momentum region due to the intraband and interband transitions of the electrons, respectively. The situation in Ge is quite similar.[8] Comparison of the present experimental data on GaAs with the theoretical data, based on the single particle model, along the [110] direction (Fig. 1) clearly shows both the effects. One should remember that the pseudo-wave-functions in our calculation lack a core-orthogonalization term and hence underestimate the high momentum region. It is hoped that the inclusion of this term will result in an increase of the high momentum

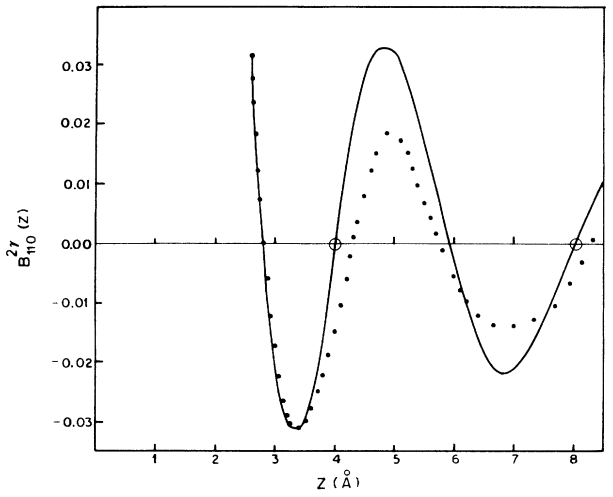

FIG. 2. Experimental (•) and theoretical (−) two-photon autocorrelation function for GaAs along the [110] direction. The circles show the lattice positions along this direction.

region and thus reveal a better picture of the dehancement effect than that seen in the present calculation.

We find in Fig. 2 that the zero crossings of the experimental AF along the [110] direction are shifted to the right of the lattice positions, whereas the theoretical AF like that derived from CP data shows zeros[16] at the exact lattice positions. We have also seen this effect in Ge (Ref. 8) and it seems to be a general feature in semiconductors. The zeros in the theoretical AF show exact values because we have used $\eta_n(\mathbf{k})$=const and the combined electron-positron wave function $[\Psi^{\pm}_{n\mathbf{k}}(\mathbf{r}) = \Psi_{n\mathbf{k}}(\mathbf{r})\Psi_{+}(\mathbf{r})]$ is periodic like the electron wave function. This effect is also seen in a recent paper on aluminum[32] where the shifting of the zero passages in the experimental AF is attributed to the electron-positron enhancement factor. It is interesting to observe however that the enhancement factor in semiconductors changes the zero positions in an opposite way to aluminum. This clearly suggests that in semiconductors a different form of enhancement factor is necessary to explain the experimental zeros.

C. Three-dimensional autocorrelation function and electron momentum density

We have used the program RECONST which uses the Fourier-Bessel transformation method to reconstruct the three-dimensional $B(\mathbf{r})$ and $\rho^{2\gamma}(\mathbf{p})$ from the measured and calculated $B(z)$.[33] This method involves the expansion of the $B(\mathbf{r})$ function in terms of the spherical harmonic functions $Y_{l,m}(\theta,\phi)$ as

$$B(\mathbf{r}) = \sum_{l,m} b_{l,m}(\mathbf{r}) Y_{l,m}(\theta,\phi). \tag{4.1}$$

Similarly $\rho^{2\gamma}(\mathbf{p})$ can be expanded in terms of the $\rho^{2\gamma}_{l,m}(\mathbf{p})$ and $Y_{l,m}(\theta,\phi)$ functions. $\rho^{2\gamma}_{l,m}(\mathbf{p})$ may be obtained from the Fourier-Bessel transform of $b_{l,m}(\mathbf{r})$ which is obtained by solving Eq. (4.1) for a number of crystallographic directions. We had experience in using RECONST with the theoretical data in order to check the convergence of $\rho^{2\gamma}(\mathbf{p})$ for the number of directions and the order of spherical harmonic functions. Like in the CP analysis[16] we find that five sets of data with four kinds of spherical harmonic functions up to eighth order are sufficient to get convergence. By omitting the term corresponding to the zeroth order of the spherical harmonic function, we have constructed the anisotropic parts $B_{\text{anis}}(\mathbf{r})$ and $\rho^{2\gamma}_{\text{anis}}(\mathbf{p})$ of $B(\mathbf{r})$ and $\rho^{2\gamma}(\mathbf{p})$, respectively.

We have plotted the theoretical and experimental $B_{\text{anis}}(\mathbf{r})$ in Fig. 3. Similarly the theoretical and experimental $\rho^{2\gamma}_{\text{anis}}(\mathbf{p})$ are plotted in Fig. 4. There is good agreement between the theoretical and experimental data in Figs. 3 and 4. Since the features seen in Figs. 3 and 4 are related to each other by the Fourier transformation, both figures carry the same physical meaning. We observe a peak at the second bond length in both the experimental and theoretical $B_{\text{anis}}(\mathbf{r})$. This corresponds to the dip seen around 1.0 a.u. in Fig. 4. Such a feature has already been seen in diamond, Si, Ge,[28] and GaAs.[16] As per the analysis of Pattison, Hansen, and Schneider[28] this feature is due to the presence of a $(4p,4p)\pi^*$ bond at the second bond length. Usually one expects to see a dip

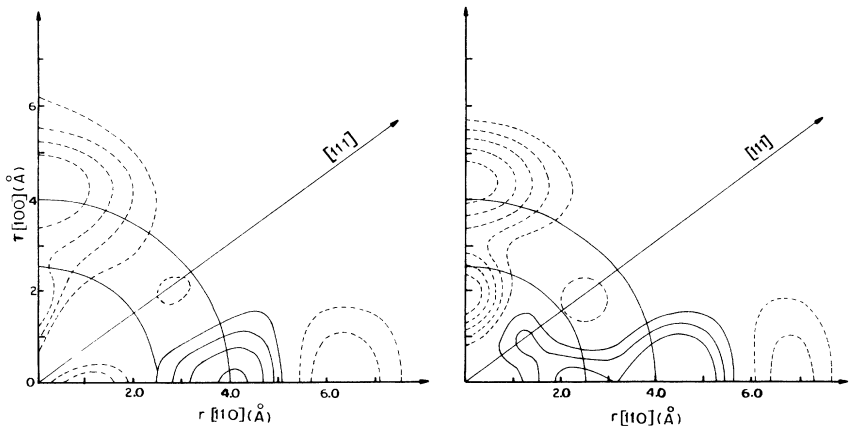

FIG. 3. Experimental (left) and theoretical (right) $B_{\text{anis}}(\mathbf{r})$ for GaAs. The contours are given in the intervals of 0.1 electrons in which the positive contours are solid and the negative contours are broken lines. Also indicated are the radial distances corresponding to the first bond length (2.45 Å) and the second neighbor bond length (4.0 Å).

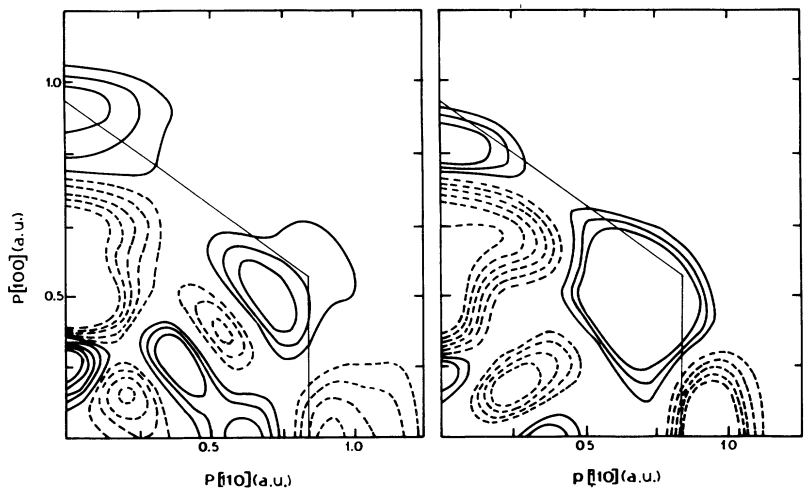

FIG. 4. Experimental (left) and theoretical (right) $\rho^{2\gamma}_{\text{anis}}(\mathbf{p})$ in GaAs. The contours are at 0.05 electrons/a.u.^{3}. The notations for the positive and negative contours are the same as in Fig. 3. The light full line denotes the Jones zone.

at the first bond length along the [111] direction in Fig. 3 due to the $(4p, 4p)\sigma$ bond effect. There is, however, no such feature seen in both the theoretical and experimental data. The failure of this analysis to observe the σ bond effect may not be surprising. The spherical average is influenced by all directional information and therefore a strong feature in some direction will also contribute to the spherical average. The effect of the positron wave function might be such that $B_{\text{anis}}(\mathbf{r})$ and $\rho^{2\gamma}_{\text{anis}}(\mathbf{p})$ have lost angular information instead of losing the radial ones.

Finally we have plotted the experimental and theoretical $\rho^{2\gamma}(\mathbf{p})$ data along the [110] direction in Fig. 5. Such an analysis generally yields a better understanding of the enhancement effect at the zone face. In fact when compared to the theoretical calculation, our experimental data show a sharper slope at the zone face. However, there are some oscillations present in the low momentum region which is not surprising. It is well known that for reasons of geometry, the long-slit apparatus does not yield accurate information about the behavior of $\rho^{2\gamma}(\mathbf{p})$ in the low momentum region.[34] The three-dimensional momentum density of Tanigawa and co-workers[13] and Liu, Berko, and Mills[35] constructed from 2D ACPAR data have clearly shown enhancement effects.

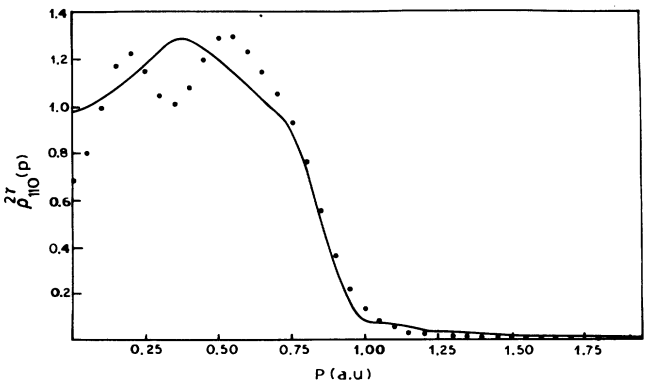

FIG. 5. Experimental (•) and theoretical (−) $\rho^{2\gamma}(\mathbf{p})$ along the [110] direction.

V. CONCLUSION

In the present work we have reported experimental and calculated ACPAR data for GaAs in different directions which agree with each other reasonably well. This has yielded a qualitative bonding picture for understanding the behavior of the data in the low momentum region. For a more quantitative representation it is required to calculate the data using a molecular orbital picture. The electron-positron enhancement and dehancement effects are discussed by comparing our experimental data with the theoretical one calculated in the single particle formalism. In metals there are many working formulas available for describing enhancement effects which when incorporated into the theoretical two-photon momentum density yield excellent agreement with the experimental data. The present work suggests the need for a working formula in semiconductors at present which does not exist. The autocorrelation anisotropy for the [111] direction is seen to be significantly changed when compared to that found in CP measurements.

ACKNOWLEDGMENTS

The author gratefully acknowledges fruitful discussions with Professor D. P. Mahapatra at different stages of this work. The author also gratefully acknowledges Dr. C. D. Beling for critically reading the manuscript.

* Present address: Department of Physics, University of Hong Kong, Hong Kong.

[1] For example, see S. Berko, *Positron Solid State Physics,* Proceeedings of the Enrico Fermi International School of Physics, "Enrico Fermi," Course LXXXIII, Varenna, 1983, edited by W. Brandt and A. Dupasquire (North-Holland, Amsterdam, 1983), p. 64

[2] J. C. Erskine and J. D. McGervey, Phys. Rev. **151**, 615 (1966).

[3] M. A. Shulman, G. M. Beardsley, and S. Berko, Appl. Phys. **5**, 367 (1975).

[4] P. U. Arifov, N. Yu. Arutyunov, V. Yu. Trashchakov, and Z. R. Abdurasulev, Fiz. Tekh. Poluprovodn. **17**, 1926 (1983) [Sov. Phys. Semicond. **17**, 1232 (1983)].

[5] D. Stroud and H. Ehrenreich, Phys. Rev. **171**, 399 (1968).

[6] H. Aourag, A. Belaidi, T. Kobayasi, R. N. West, and B. Khelifa, Phys. Status Solidi B **156**, 497 (1989).

[7] R. N. West, J. Mayers, and P. A. Walters, J. Phys. E **14**, 478 (1981).

[8] B. K. Panda and D. P. Mahapatra, J. Phys. Condens. Matter **5**, 3475 (1993).

[9] H. Aourag, B. Khelifa, A. Belaidi, and Z. Belarbi, Phys. Status Solidi B **160**, 201 (1990).

[10] B. K. Panda, D. P. Mahapatra, H. C. Padhi, K. P. Gopinathan, C. S. Sundar, and G. Amarendra, J. Phys. C **22**, 6039 (1988); B. K. Panda, D. P. Mahapatra, and H. C. Padhi, Phys. Status Solidi B **167**, 133 (1991).

[11] B. K. Panda, D. P. Mahapatra, and H. C. Padhi, Phys. Status Solidi B **169**, 89 (1992).

[12] N. Yu. Arutyunov, Mater. Sci. Forum **105-110**, 583 (1992).

[13] S. Tanigawa, Mater. Sci. Forum **105-110**, 493 (1992); H. Kondo, Y. K. Cho, T. Kubota, T. Kawano, K. Watanabe, and S. Tanigawa, J. Phys. Condens. Matter **4**, 5911 (1992); M. Saito, A. Oshiyama, and S. Tanigawa, Phys. Rev. B **44**, 10 601 (1991); Y. K. Cho, H. Kondo, T. Kubota, H. Nakashima, T. Kawano, and S. Tanigawa, Mater. Sci. Forum **105-110**, 615 (1992); Y. K. Cho, H. Kondo, T. Kubota, H. Nakashima, T. Kawano, and S. Tanigawa, *ibid.* **105-110**, 619 (1992).

[14] N. Sakai, N. Shiotani, F. Itoh, O. Mao, M. Ito, H. Kawata, Y. Amemiya, and M. Ando, J. Phys. Soc. Jpn. **58**, 3270 (1989).

[15] H. Nara, K. Shindo, and T. Kobayashi, J. Phys. C **11**, 3967 (1984).

[16] D. N. Timms, M. J. Cooper, R. S. Holt, F. Itoh, T. Kobayashi, and H. Nara, J. Phys. Condens. Matter **2**, 10 517 (1990).

[17] G. Dlubek and R. Krause, Phys. Status Solidi A **102**, 443 (1987).

[18] B. K. Panda, H. C. Padhi, and B. Viswanathan, in *Positron Annihilation and Compton Scattering,* edited by B. K. Sharma, R. M. Singru, and P. C. Jain (Omega Scientific Publishing, New Delhi, 1990), p. 169.

[19] P. E. Mijnarends, in *Positrons in Solids*, edited by P. Hautojärvi, Topics in Current Physics Vol. 12 (Springer-Verlag, Berlin, 1979), p. 25, and references therein.

[20] K. P. Gopinathan, C. S. Sundar, B. Viswanathan, and A. Bharathi, Bull. Mater. Sci. **2**, 207 (1980).

[21] T. Chiba and N. Tsuda, Appl. Phys. **5**, 37 (1974).

[22] For example, see M. L. Cohen and J. R. Chelikowsky, in *Electronic Structure and Optical Properities of Semiconductors*, edited by M. Cardona (Springer-Verlag, Berlin, 1988).

[23] J. R. Chelikowsky and M. L. Cohen, Phys. Rev. B **14**, 556 (1976).

[24] H. Rojas, B. Barbiellini, and T. Jarlborg, Mater. Sci. Forum **105-110**, 799 (1992).

[25] The representation of the data through $B(\mathbf{r})$ has several advantages over $N(p_z)$. It is conceptually simpler to interpret experimental results in position space rather than in momentum space. The isotropic core-electron contribution and most residual systematic errors which are all slowly varying functions of momentum are restricted to a small region around the origin in $B(\mathbf{r})$. The size and sign of the B function may under certain circumstances provide the information about the type of bonding between different elements in an atomic chain. P. Pattison and W. Weyrich, J. Phys. Chem. Solids **40**, 213 (1979).

[26] W. Schülke, Phys. Status Solidi B **82**, 229 (1977). The measured zero crossings will be unaffected by the isotropic core contributions, resolution function, and most residual systematic errors.

[27] D. J. Chadi and M. L. Cohen, Phys. Rev. B **8**, 5747 (1973).

[28] P. Pattison, N. K. Hansen, and J. R. Schneider, Chem. Phys. **59**, 231 (1981).

[29] S. T. Pantelides and W. A. Harrison, Phys. Rev. B **11**, 3006 (1975).

[30] S. Berko, R. E. Kelley, and J. S. Plaskett, Phys. Rev. **106** 824 (1954).

[31] K. Fujiwara, T. Hyodo, and J. Ohyama, J. Phys. Soc. Jpn. **33**, 1047 (1972); K. Fujiwara and T. Hyodo, *ibid.* **35**, 1133 (1973).

[32] B. K. Panda, Phys. Status Solidi B **170**, 481 (1992).

[33] N. K. Hansen, P. Pattison, and J. R. Schneider, Z. Phys. B **66**, 305 (1987); N. K. Hansen (unpublished).

[34] P. E. Mijnarends, Phys. Rev. **178**, 622 (1969).

[35] W. Liu, S. Berko, and A. P. Mills, Mater. Sci. Forum **105-110**, 743 (1992).